In Fig. 1, the theoretical (——)sputtering rates $S(E)$ are plotted in dependence of energy $E_0 < E \leq 100$ eV for Hg ions, and W and Mo targets. For comparison, the corresponding experimental (– – –) sputtering ratios $S(E)$ as measured by Askerov and Sena[7] are shown, which represent the most reliable sputtering data presently available. It is seen that the agreement between theory and experiment is very satisfactory for energies E close to the threshold E_0. In view of the approximations made, it is clear that the theoretical and experimental $S(E)$ values must deviate more and more for increasing E. A better agreement between theory and experiment could possibly be achieved if the cross sections and their energy dependence were known accurately.

The main purpose of the simplified analysis presented is to demonstrate that the underlying idea of the phase space dynamics leads to sputtering ratios which agree approximately with the experimental observations. The theory can be extended and improved by considering additional effects and interactions as will be shown in a later publication.

References

[1] Behrisch, R., *Ergebn. Exakt. Naturw.* Vol 35, 1964, pp. 295-443.

[2] Stuart, R.V. and Wehner, G.K., *Journal of Applied Physics,* Vol. 33, 1962, pp. 2345-2352.

[3] Beebe, D.D., Nakanishi, S., and Finke, R.C., TM X-3044, 1974, NASA.

[4] Staggs, J.F., Gula, W. P., and Kerslake, W.R., *Journal of Spacecraft* Vol. 5, 1968, pp. 159-164.

[5] Kohlraush, F., *Practical Physics, III,* B.G. Teubner, Stuttgart, Germany 1968.

[6] Mott, N.F. and Massey, H.S.W., *The Theory of Atomic Collisions, Oxford University Press,* Oxford, Eng., 1965.

[7] Askerov, Sh. G. and Sena, L.A., Soviet Physics—*Solid State,* Vol. 11, 1969, pp. 1288-1292.

Roughness Induced Transition Criteria for Space Shuttle-Type Vehicles

E. Leon Morrisette*

NASA Langley Research Center, Hampton, Va.

Nomenclature

b	= semispan
M_c, M_p	= local Mach number on cone and flat plate, respectively
P	= pressure
P'	= longitudinal pressure gradient
r	= blunt body nose radius
R_k	= Reynolds number based on boundary-layer edge conditions at roughness and roughness height
$R_{x,k}$	= Reynolds number based on boundary layer edge conditions and x_k
T	= temperature
x	= longitudinal surface distance from stagnation point
x_k	= value of x at roughness location
y	= spanwise distance from centerline of body
Subscripts	
aw	= adiabatic wall
eff	= effective
t	= total
w	= wall

Received July 16, 1975; revision received December 1, 1975.

Index categories:

*Aerospace Engineer, Applied Fluid Mechanics Section, High-Speed Aerodynamics Division.

WHILE criteria exist for determining the size of three-dimensional surface roughness which will promote boundary-layer transition on simple geometric shapes,[1-3] the criteria are ill-defined for configurations with significant longitudinal and/or lateral pressure gradients (cross flow). Design of the space shuttle requires this information for sizing trips for wind-tunnel tests and for determining the effect of roughness on vehicle performance. This Note compares tripping effectiveness of roughness on a delta wing shuttle orbiter model at 20° angle of attack to that on plane and axisymmetrical bodies with and without longitudinal pressure gradients.

Two prominent parameters used in correlations of roughness induced transition are critical roughness Reynolds number[4] and effective roughness Reynolds number.[2] Critical roughness Reynolds number is a function of the flow conditions between the roughness and the "natural" transition location and probably of freestream noise. The experimental data herein are compared on the basis of effective roughness Reynolds number since this parameter is not sensitive to flow conditions downstream of the roughness. It is also believed that the effect of tunnel freestream noise on the parameter is negligible since the roughness induced disturbance dominates the transition process.[5] The effective roughness size is the smallest size roughness which causes transition to move very close to the roughness element. A compilation of effective roughness Reynolds numbers (transformed to adiabatic wall conditions) for zero pressure gradient, two-dimensional and axisymmetric flows is shown in Fig. 1 as a function of $R_{x,k}$ for various Mach numbers (faired lines, not symbols). The data were transformed to adiabatic wall conditions by using a ratio form of an equation given by Van Driest[2] which empirically accounts for the effect of wall cooling on effective roughness size

$$\frac{R_{k,eff}}{R_{k,eff,aw}} = 1 - .81 \left[\frac{T_{aw}}{T_t} - \frac{T_w}{T_t} \right] \tag{1}$$

A substantial increase in the effective roughness Reynolds number above those in zero pressure gradient at the same local flow conditions is obtained on blunt flat plates, cones, and the centerline of the shuttle model (symbols, Fig. 1, Table 1).

This effect of pressure gradient is better shown in Fig. 2. While the size parameter ratio is obviously a function of more than just pressure gradient, the effective roughness Reynolds number increases nearly an order of magnitude in the region of high-pressure gradient. The data in Fig. 2b show the same trend and allow comparison of data for which the magnitude of the pressure gradient is not available (such as the present orbiter data). The data of Fig. 2a and 2b should be considered as indicating trends and not magnitude because of the significant interpolation and extrapolation of the zero

Table 1 Key for Figs. 1 and 2

Key for figures 1 and 2					
Symbol	Configuration	M_∞	x/r	$\frac{dP}{dx}, \frac{psi}{in}$	Ref.
○	Blunt flat plate	6.0	46.0	-2.37×10^{-2}	11
○	Blunt flat plate	6.0	15.4	-2.93×10^{-2}	11
○	Blunt flat plate	6.0	15.4	-4.22×10^{-2}	11
□	Blunt cone	10.16	0.785	-3.33	9
□	Blunt cone	10.16	1.12	-1.94	9
□	Blunt cone	10.16	1.47	-0.903	9
◇	Blunt cone	10.16	0.785	-9.72	9
◇	Blunt cone	10.16	1.12	-5.89	9
◇	Blunt cone	10.16	1.47	-1.89	9
▽	Blunt cone	8.0	13.0	-1.24×10^{-2}	10
▽	Blunt cone	8.0	20.4	$+8.00 \times 10^{-4}$	10
△	Delta-wing orbiter	6.0	9	-	Present study
△	Delta-wing orbiter	6.0	18	-	Present study

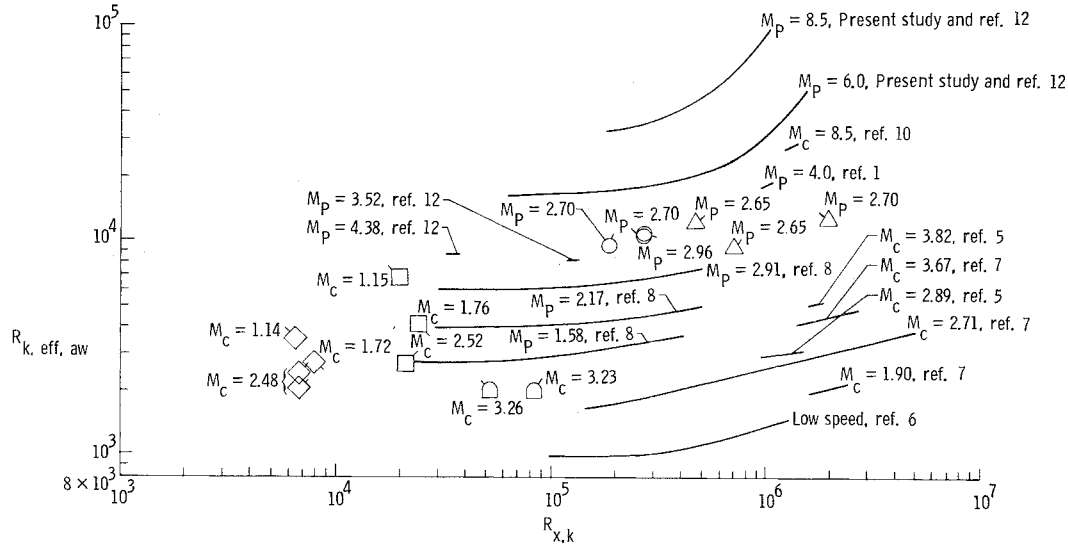

Fig. 1 Effective roughness Reynolds number as a function of roughness position Reynolds number.

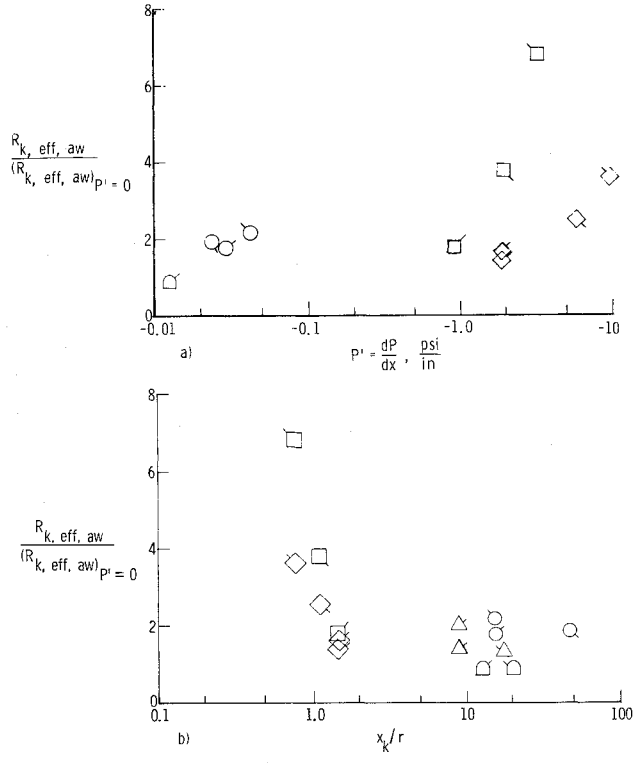

Fig. 2 Effect of longitudinal pressure gradient on $R_{e,eff}$ (blunt cones and plates). a) effective size ratio as a function of pressure gradient; b) effective size ratio as a function of distance from vehicle nose.

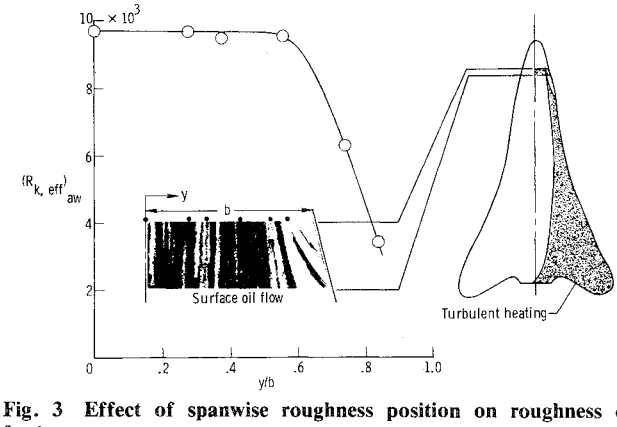

Fig. 3 Effect of spanwise roughness position on roughness effectiveness.

pressure gradient curves (Fig. 1) necessary to obtain values of effective roughness Reynolds number. The data in Figs. 2a and 2b are all for favorable pressure gradient since the only adverse pressure gradient data available is in a gradient so weak as to have no appreciable effect on effective roughness size.

While the orbiter centerline data agree with the other blunt body data (Fig. 2), effective roughness Reynolds numbers obtained at off-centerline locations are more strongly effected by the cross-flow pressure gradients. As shown in Fig. 3, $R_{k,\,eff}$ rapidly decreases near the shoulder of the model where the cross flow becomes significant. The cross flow is illustrated by the surface oil flow picture shown in the insert of Fig. 3; the curvature of the oil streaks indicates a direct relationship between the point of decreasing effective roughness size and the beginning of severe cross flow. This is somewhat contradictory to the conclusions drawn from Fig. 2, that favorable pressure gradient increases $R_{k,eff}$ (i.e., the high cross flow in Fig. 3 is the result of a severe favorable pressure gradient in the traverse plane). The cross flow itself may be unstable and require a smaller disturbance to initiate transition. Also, the cross flow reduces the local boundary-layer thickness, making the flow more sensitive to roughness. The use of calculated centerline boundary-layer edge conditions to calculate the Reynolds numbers for the roughness near the shoulder may be in error, but the conclusion remains that much smaller roughness is required near the shoulder to promote transition.

The right side of Fig. 3 shows the experimental extent of turbulent heating downstream of one roughness element (slightly smaller than effective) near the vehicle shoulder ($y/b = 0.75$). The spread of turbulence results in nearly one-third of the planform area being immersed in turbulent flow. On a flight vehicle, this may cause a severe increase in the overall surface heating, as well as flight stability problems since one control flap may have laminar flow while the other has turbulent flow.

This Note has shown that conventional criteria for sizing roughness elements which promote transition in two-dimensional zero pressure gradient flows are insufficient for high-pressure gradient flows and three-dimensional flows. In addition roughness much smaller than that given by conventional criteria can cause transition and significantly increase the heating load.

References

[1] Potter, J.L. and Whitfield, J.D. "Effects of Unit Reynolds Number Nose Bluntness, and Roughness on Boundary Layer Transition," TR-60-5, March 1960, Arnold Engineering Development Center, Tullahoma, Tenn.

[2] Van Driest, E.R. and Blumer, C.B. "Summary Report on Studies on Boundary Layer Transition for Years 1963-64," SID64-2191, Dec. 1964, Space Sciences Lab., North American Aviation, Inc., Space and Information Systems Div.

[3] Braslow, A. L. Knox, E.C., and Horton, E. A. "Effect of Distributed Three-Dimensional Roughness and Surface Cooling on Boundary Layer Transition and Lateral Spread of Turbulence at Supersonic Speeds," TN D-53, 1959, NASA.

[4] Gibbings, J.C. and Hall, J.D., "Criterion for Tolerable Roughness in a Laminar Boundary Layer," *Journal of Aircraft*, Vol. 6, March-April 1969, pp. 171-173.

[5] Pate, S.R., "Induced Boundary Layer Transition at Supersonic Speeds: Combined Effects of Roughness and Free Stream Disturbances," *AIAA Journal*, Vol. 9, May 1971, pp. 797-803.

[6] Klebanoff, P.S., Schulbauer, G.B., and Tidstrom, K.D., "Measurements of the Effect of Two-Dimensional and Three-Dimensional Roughness Elements on Boundary-Layer Transition," *Journal of the Aeronautical Sciences*, Vol. 22, Nov. 1955, pp. 803-804.

[7] Van Driest, E.R. and McCauley, W.D., "The Effect of Controlled Three-Dimensional Roughness on Boundary Layer Transition at Supersonic Speeds," *Journal of the Aerospace Sciences*, Vol. 27, April 1960, pp. 261-271. 303.

[8] Hicks, R.M. and Harper, E.R., Jr., "A Comparison of Spherical and Triangular Boundary Layer Trips on a Flat Plate at Supersonic Speeds," TM X-2416, 1970, NASA.

[9] McCauley, W.D., Saydah, A.R., and Beuche, J.F., "Effect of Spherical Roughness on Hypersonic Boundary Layer Transition, *AIAA Journal*, Vol. 4, Dec. 1966, pp. 2142-2148.

[10] Stainback, P. C., "Effect of Unit Reynolds Number, Nose Bluntness, Angle of Attack and Roughness on Transition on a 5°Half-Angle Cone at Mach 8, " TN D-4961, 1969, NASA.

[11] Holloway, P. F. and Morrisette, E. L., "Roughness Effects on Boundary Layer Transition for Blunt-Leading-Edge Plates at Mach 6," TN D-3517, 1966, NASA.

[12] Morrisette, E.L., Stone, D.R., and Whitehead, A.H., Jr. Boundary-Layer Tripping with Emphasis on Hypersonic Flows," *Presented at the Symposium on Viscous Drag Reduction*. Dallas, Texas, September 24 and 25, 1968. Sponsored by ONR and NASA.

Atmospheric Entry into Jupiter's Atmosphere in View of Recent Flyby Results

Philip R. Nachtsheim,* Edward Tindle,†
and
John T. Howe‡
NASA Ames Research Center, Moffett Field, Calif.

Nomenclature

A	= frontal cross sectional area of probe
C_D	= drag coefficient
g	= gravitational constant
m	= probe mass
q	= heating rate
R	= universal gas constant
R_N	= nose radius
t	= time
T	= temperature
V	= probe velocity
y	= distance above reference altitude
ρ	= gas density

Subscripts

conv	= convective
E	= entry condition
0	= pertains to a reference altitude
rad	= radiative
∞	= ambient flight condition

Received July 21, 1975; revision received October 14, 1975.

Index categories: Entry Vehicles; Radiation and Radiative Heat Transfer.

*Assistant Chief, Thermal Protection Branch, T&G Division. Member AIAA.

†Research Scientist, Space Exploration Branch, Systems Study Division.

‡Research Scientist, Thermal Protection Branch, T & G Division. Member AIAA.

Introduction

TEMPERATURE profiles of Jupiter's atmosphere, based on the data of the Pioneer 10 occultation experiment,[1,2] indicate that the atmosphere is much warmer than was previously thought. These results by Kliore et al., are not in agreement with Earth-based observations of the Jovian atmopshere,[3-5] nor with the results of the Pioneer 10 infrared experiment of Munich.[6] Nonetheless, the implications of Kliore's preliminary results are of interest because of the generally held belief that entry into a warmer atmosphere would produce less aerodynamic heating of an entry probe. And any lessening of the extreme heat levels that a Jupiter probe is expected to encounter could permit a significant reduction in heat shield weight and a corresponding increase in science payload.

This paper examines the heating levels experienced by a probe entering the "Kliore" model atmosphere and compares the results with those of the Jupiter model atmospheres given in Ref. 7, with the heating levels of Tauber[8] and Tauber and Wakefield.[9] The computations made in this paper employ a point-mass atmopsheric entry trajectory program, that is, the Allen-Eggers analysis[10] and simple correlations of heating. First the atmospheres are identified and then the atmospheric entry analysis is given along with the heating correlations. The result of the heating calculations are compared and discussed.

Atmospheric Heating and Entry into Model Atmospheres of Jupiter

The Kliore model atmosphere is compared with the model atmospheres of Jupiter obtained from Ref. 7 in Fig. 1. Results inferred from the other Pioneer 10 experiments and Earth-based observations are also shown. It is seen that the Kliore atmosphere is distinguished by a temperature bulge at about 200 K.

A simplified entry analysis with constant probe mass probably would not significantly change the relative relations among the heating values for the various model atmospheres. The factors that influence the heating of the probe during deceleration are the atmospheric composition and scale height. The Kliore measurements give no direct measure of the composition. He assumed a composition of 85% hydrogen and 15% helium by number, and found the atmospheric model was insensitive to the assumed composition. At any given altitude the scale height is determined by the temperature at that altitude, and the density variation is given by

$$\rho_\infty = \rho_0 \exp\left[-\frac{Mg}{RT}\, y\right] \tag{1}$$

The probe deceleration can be described by the expression

$$dV_\infty/dt = -\frac{C_D A}{m}\, \tfrac{1}{2}\rho_\infty V_\infty^2 \tag{2}$$

Apart from the ballistic coefficient, $m/C_D A$, it is seen that the deceleration is influenced mainly by the time variation of the density ρ_∞ as the probe decelerates in the atmosphere. The